



# Towards accurate measurements of specific heat of solids by drop calorimetry up to 3000 °C

Refat Razouk, Olivier Beaumont, Jacques Hameury, Bruno Hay

## ► To cite this version:

Refat Razouk, Olivier Beaumont, Jacques Hameury, Bruno Hay. Towards accurate measurements of specific heat of solids by drop calorimetry up to 3000 °C. Thermal Science and Engineering Progress, 2021, 26, pp.101130. 10.1016/j.tsep.2021.101130 . hal-03653147

**HAL Id: hal-03653147**

**<https://cnam.hal.science/hal-03653147>**

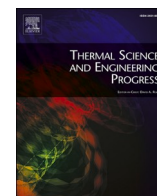
Submitted on 27 Apr 2022

**HAL** is a multi-disciplinary open access archive for the deposit and dissemination of scientific research documents, whether they are published or not. The documents may come from teaching and research institutions in France or abroad, or from public or private research centers.

L'archive ouverte pluridisciplinaire **HAL**, est destinée au dépôt et à la diffusion de documents scientifiques de niveau recherche, publiés ou non, émanant des établissements d'enseignement et de recherche français ou étrangers, des laboratoires publics ou privés.



Distributed under a Creative Commons Attribution - NonCommercial - NoDerivatives 4.0  
International License



# Towards accurate measurements of specific heat of solids by drop calorimetry up to 3000 °C

Refat Razouk<sup>\*</sup>, Olivier Beaumont, Jacques Hameury, Bruno Hay

Laboratoire National de Metrologie et d'Essais, Laboratoire Commun de Metrologie (LNE-LCM), Scientific and Industrial Metrology Centre, 1 rue Gaston Boissier, 75015 Paris, France

## ARTICLE INFO

**Keywords:**  
Drop calorimetry  
Specific heat  
High temperature  
Metrology

## ABSTRACT

The French National Metrology Institute LNE-LCM has modified a high temperature Laser Flash apparatus in order to perform the measurement of the specific heat of solids by drop calorimetry. A sample hanging on a thin wire held by a motorised gripper, is heated by the inductive furnace and dropped into a heat-flux Calvet calorimeter maintained at near ambient temperature. The calorimeter is equipped with an *in-situ* electrical calibration system in order to perform accurate and reliable measurements of energy directly traceable to the International System of Units (SI). The electrical calibration system has been designed for the calibration of the calorimeter by electrical substitution (Joule effect) and remains *in-situ* during the drop of the heated sample, keeping exactly the same experimental configuration during both steps of calibration and measurement. The metrological features (sensitivity, linearity) of the calorimeter have been evaluated by investigating the influence of the level of energy and dissipation time on the determination of the sensitivity factor of the heat-flux calorimeter. A calibration and measurement procedure was established in order to enable the measurement of the enthalpy increments of solids up to 2700 °C. The first results obtained for the determination of the specific heat of  $\alpha$ -alumina (SRM-720), tungsten and graphite, as well as for the measurements of the enthalpy of fusion of pure copper are in good agreement with literature values and a relative uncertainty of 5% can be obtained.

## 1. Introduction

Drop calorimetry [1,2] is an old technique for the quantification of the heat released by a sample when it is heated at a known temperature and then dropped into a receiving calorimeter. In many apparatuses, the initial specimen temperature is greater than the calorimeter's one which is usually maintained around room temperature, or at the ice point (like Bunsen type ice calorimeter [3]). The calorimeter measures the heat evolved in cooling the sample to the calorimeter temperature. In some other cases, the sample is maintained at near room temperature and dropped in a heated calorimeter in order to quantify how much heat the specimen "absorbs" to reach the calorimeter temperature [4]. The limitation of this second type of drop-calorimeters is the development of heat-flux sensor with sufficient sensitivity and low noise level at high temperatures [5].

In conventional drop calorimetry where the sample is heated in a furnace then dropped in a calorimeter, the main sources of uncertainty are associated with temperature measurement and the attainment of equilibrium in the furnace, the evaluation of heat losses during drop, the

measurement of the heat released in the calorimeter, and the reproducibility of the initial and final states of the sample [6]. At high temperatures, chemical reactions between the sample and the container can lead to serious uncertainties. They may be avoided by either electromagnetic levitation of the sample in a vacuum furnace [7], or by aerodynamic levitation [8].

Despite the development of different measurement techniques for thermophysical properties measurements, accurate measurement of specific heat above 1500 °C remains a very challenging experimental issue. But the derivation of specific heat from enthalpy data obtained with drop calorimetry remains the most reliable method [9].

The French National Metrology Institute LNE-LCM has developed a Laser Flash Apparatus (LFA) [10] for the measurement of the thermal diffusivity of solids by the laser flash method [11] from ambient temperature up to 3000 °C. In the framework of the European project EMPIR 17IND11 Hi-TRACE [12], the LNE-LCM works on the development of a metrological reference facility for traceable measurements of the specific heat of solid materials at high temperatures (up to 3000 °C). The chosen approach is based on measurements of enthalpy increments by

<sup>\*</sup> Corresponding author.

E-mail address: [refat.razouk@lne.fr](mailto:refat.razouk@lne.fr) (R. Razouk).

<https://doi.org/10.1016/j.tsep.2021.101130>

Received 29 July 2021; Received in revised form 29 October 2021; Accepted 30 October 2021

Available online 8 November 2021

2451-9049/© 2021 The Authors.

Published by Elsevier Ltd.

This is an open access article under the CC BY-NC-ND license

(<http://creativecommons.org/licenses/by-nc-nd/4.0/>).

the drop calorimetry method where the tested specimen is heated in the inductive furnace of the diffusivimeter and dropped in a heat-flux calorimeter at room temperature. Different elements were added to the LFA in order to adapt it for the measurement of specific heat of solids at high temperatures, keeping the possibility to switch between thermal diffusivity and specific heat measurements using the same set-up.

## 2. Description of the drop-calorimeter set-up

The new drop-calorimeter, presented in Fig. 1, was developed using an existing induction furnace incorporated in a high-temperature laser-flash diffusivimeter presented in [10]. For specific heat measurements, the induction furnace is equipped at the top with a motorised gripper and with a differential heat-flux calorimeter at the bottom to receive the specimen heated in the furnace. The enthalpy increment measured by the calorimeter corresponds to the cooling of the sample from the initial temperature in the furnace to the temperature of the calorimeter.

The specimen is placed inside the induction furnace in a container suspended from a thin wire held by an automated gripper. The temperature of the specimen is measured using optical pyrometers covering the range from 500 °C up to 3000 °C. The pyrometers “see” the bottom face of the container through a periscope made of a flat silver mirror inclined at 45° and held between the furnace and the calorimeter on a horizontally motorised translator. Once the temperature of the specimen is measured after stabilisation, the deflection mirror translates in order to let the specimen drop in the calorimeter for enthalpy measurement. The different elements of the drop calorimeter are described herein after in addition to a brief description of the measurement method.

### 2.1. Differential heat flux calorimeter

The calorimeter is composed of two Calvet [13,14] thermopiles plugged in a thermalized cylindrical massive block of aluminum. The block is stabilised at near room temperature (25 °C) using temperature regulated water circulation in a jacket around the block. The schematic drawing of the calorimeter is presented in Fig. 2.

Each thermopile delivers a voltage proportional to the heat flux from the cell inside the fluxmeter to the aluminum block. The thermopiles of the two fluxmeters are electrically connected in opposition in order to

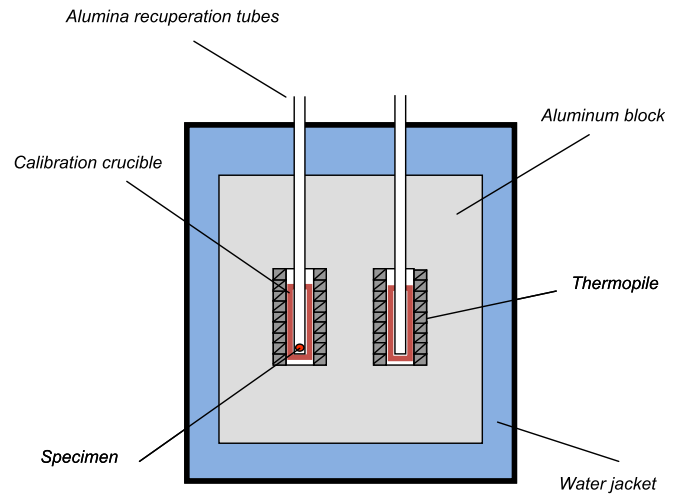


Fig. 2. Schematic of the calorimeter.

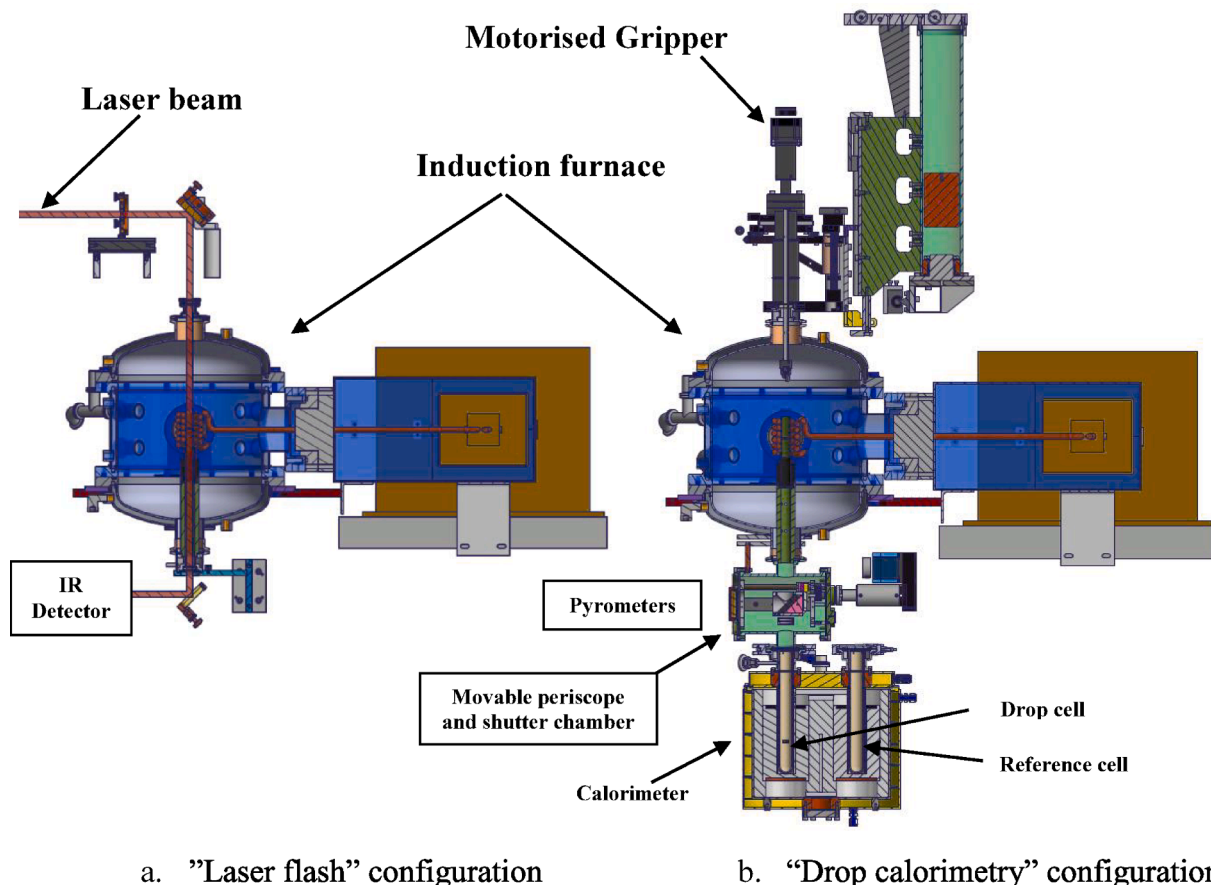


Fig. 1. LNE-LCM set-up for thermal diffusivity and specific heat measurements at high temperatures.

compensate the parasitical heat fluxes due to any temperature fluctuation of the block. Indeed, the electromotive force (EMF) generated by the arrangement of two fluxmeters connected in opposition is proportional to the difference between the heat fluxes dissipated in the two cells. A calibrated resistance temperature sensor (Pt-100) measures the mean temperature of the aluminum block. Two identical high density and air tight alumina tubes, closed at one end and equipped with a protection material of tungsten or graphite inside, are inserted in the calorimeter cells. The protection materials protect the alumina tubes from the high temperature of the dropped specimens. The upper open ends of the tubes are hermetically connected to the furnace through the intermediate chamber containing a movable periscope and a shutter (in Fig. 1).

When a heated specimen is dropped in the “sample” cell, it transfers its heat to the aluminum block through the thermopile of the “sample fluxmeter”. The electrical signal  $S(t)$  delivered by the two fluxmeters connected in opposition is measured as a function of time  $t$ . The time integration of this signal divided by the sensitivity coefficient  $\beta$  of the thermopiles (expressed in  $\mu\text{V}\cdot\text{W}^{-1}$ ) gives the heat released by the specimen in the calorimeter. The accuracy of the energy measurements is therefore directly dependent on the determination of the sensitivity coefficient of the calorimeter.

An in-situ electrical calibration system enabling to perform the heat calibration of the calorimeter by Joule effect was developed in order to prevent any modification of the experimental conditions during measurement. An acquisition system with calibrated devices has been assembled in order to perform accurate and traceable measurements.

This calibration system consists in a resistance heating wire of nickel-chromium alloy (Ni80/Cr20), having an electrical resistivity of  $1.08 \times 10^{-6} \Omega\cdot\text{m}$ , wound on a length of 60 mm around an alumina crucible of 30 mm external diameter and 90 mm long (cf. Fig. 3a). The heating wire has a diameter of 0.25 mm, and is connected from the upper part of the crucible in 4-wire configuration to a programmable DC power supply (Keithley 2200) and a digital multimeter (HP 34970A). This multimeter measures the voltage drops across the heating wire as well as across a standard resistance of  $0.1 \Omega$ , installed in series with the heating wire for accurate current measurement. Copper wires are used for current supply and voltage measurement at the upper part of the calibration crucible. These wires exit the calorimeter through a special gas-tight connector (cf. Fig. 3b).

A calibrated multimeter (Agilent 34970A) measures the electromotive force delivered by the thermopiles and the resistance of the Pt-100 in addition to voltage drops over the heater and the standard resistance. A computer runs a Labview program that controls and synchronises both the electrical power dissipation in the heating wire and the data acquisition by the digital multimeter. The multimeter, the standard resistance as well as the time base of the computer have been calibrated. An identical calibration system is put in each alumina tube in order to keep the thermal symmetry of the two cells. Only the calibration system, in which the specimen is supposed to drop, is connected to the power supply and to the digital multimeter HP 34970A.

The calibration of the calorimeter consists in releasing a known amount of energy in the drop cell, and in recording the response of the thermopiles versus time. More details of the calibration procedure can be found in papers [15,16].

## 2.2. Mechanical parts

### 2.2.1. Motorised gripper

The sample container is held by a motorised gripper (presented in Fig. 1) using a thin wire of tungsten or tantalum (diameter of 50  $\mu\text{m}$ , or 100  $\mu\text{m}$ ). The wire is pinched in the groove of the gripper which can be aligned manually along the axis of the furnace and of the sample cell of the calorimeter. The drop of the sample is controlled by the Labview program which synchronizes the movements of the elements (gripper, deflection mirror and shutter).

### 2.2.2. Induction furnace

The specimen inside the container is heated by a graphite susceptor which is itself heated by the copper inductive coil of the furnace. The type of the furnace is CELES MP50/400 with a nominal power of 50 kW.

### 2.2.3. Intermediate chamber with movable periscope and movable shutter

The intermediate chamber contains the movable deflection mirror and the movable shutter which reduces the heat fluxes by radiation from the hot elements in the furnace toward the sample cell of the calorimeter.

The deflection mirror is inclined at  $45^\circ$  in order to enable the pyrometers to measure the temperature of the sample container through a

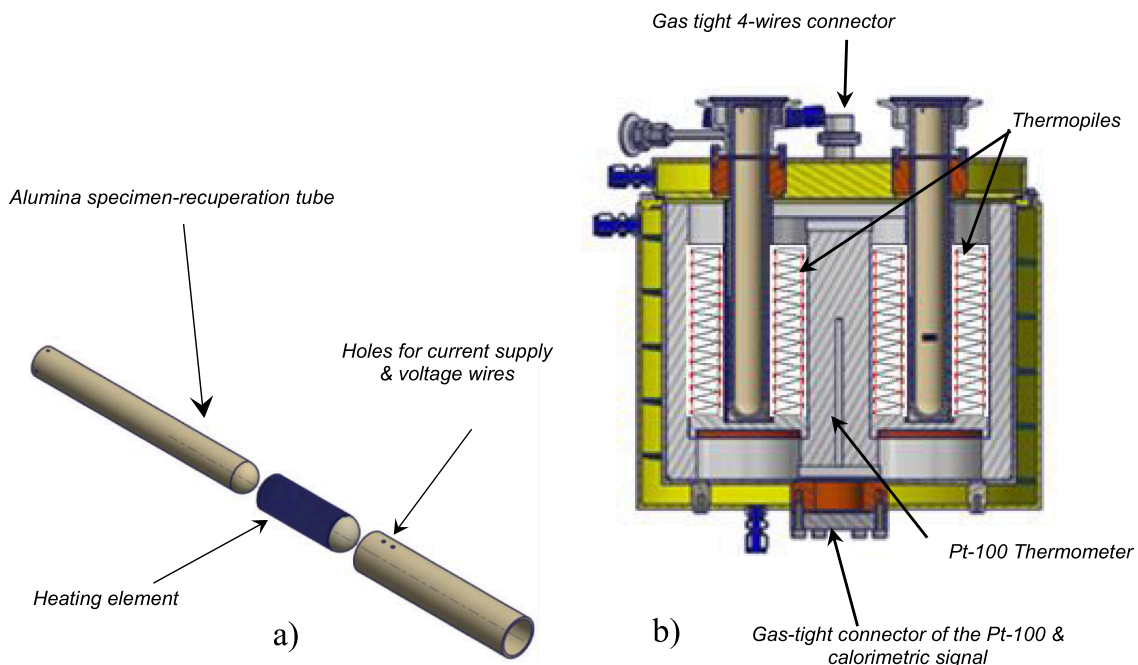


Fig. 3. Design of the electrical calibration crucible.

50 mm diameter uncoated barium fluoride ( $\text{BaF}_2$ ) window. The mirror can move along a horizontal axis. The shutter is placed just below the mirror. The shutter is composed of a circular water-cooled thick metallic mirror that covers the entire opening of the sample cell. It is switched when the sample container is released by the gripper letting the sample and the container drop into the calorimeter sample cell. Just after the container is in the sample cell, the shutter is switched back to the position above the sample cell. The shutter and deflection mirror movements are controlled by the Labview program.

#### 2.2.4. Specimen container

Different specimen containers are used; they are made of tungsten, tantalum or graphite depending on the material tested. The design of the specimen container is presented in Fig. 4. The design accepts specimens of maximum 5 mm in diameter and 20 mm height. The specimen container is not airtight, and it is supposed that it is filled with helium (the same atmosphere during the drops).

#### 2.3. Temperature measurement of the specimen heated in the induction furnace

Over 1000 °C, the specimen's temperature is measured by a bi-color pyrometer (IMPAC infratherm ISQ 5) that operates from 1000 °C to 3000 °C. The pyrometer was initially calibrated for measurement of radiance temperature with reference black body sources in a National Metrology Laboratory.

### 3. Principle of the specific heat measurement by the drop method

The principle of drop calorimetry (from hot to cold temperature) is described in details in [1,2] and in different scientific papers [9].

When a container containing a specimen, both heated in the furnace, drops in the calorimeter maintained at near room temperature, the time integration of the signal  $S(t)$  delivered by the calorimeter as a function of the time  $t$ , divided by the sensitivity coefficient  $\beta$  of the calorimeter gives the enthalpy variation of the container and specimen between the initial temperature in the furnace and the temperature of the calorimeter.

Two successive drops are performed for each temperature level, one with the container empty and another one with the container and the

specimen. The sample is easily removed after each drop. The enthalpy measurement with the empty container allows to compensate heat losses during the drop and to correct the results from the influence of the container. The assumption is that the heat losses during the drop are identical with the empty container or with the container with the sample.

The curve of the enthalpy increments as a function of the temperature is obtained by keeping constant the temperature of the calorimeter ( $T_0$ ), and performing different drops with different temperatures of the container and sample in the furnace.

Knowing the mass of the sample ( $m$ ), determined using a calibrated balance, the enthalpy variation of the sample between the two thermodynamic states (identified by the temperature of the sample  $T$ , and the temperature of the calorimeter  $T_0$ ) is given by equation (1).

$$\Delta H(T) = n \int_{T_0}^T c_p(T) \cdot dT \quad (1)$$

With  $n$  the number of mols ( $n = m/M$ ), and  $M$  the molecular weight of the material.

The specific heat at a given temperature can be derived from the smoothed enthalpy increment results by differentiation as given by equation (2).

$$c_p(T) = \frac{1}{n} \left( \frac{d\Delta H(T)}{dT} \right)_p \quad (2)$$

The mathematical models used for fitting enthalpy increments (expressed in Joule) of empty and full containers versus temperature are given by equation (3).

$$H(T) - H_{298.15} = A + B \cdot T + C \cdot T^2 + \frac{D}{T} \quad (3)$$

with  $T$  the temperature in K.

The difference between the enthalpy increments of full and empty container, which represent the enthalpy increments of only the sample, are modelled [21,22] with a similar mathematical model taking into account boundary conditions. Differentiating this equation and taking into account the mass of the sample leads to the following relationship giving the specific heat as a function of temperature.

$$c_p(T) = \frac{1}{n} \left( B + 2C \cdot T - \frac{D}{T^2} \right) \quad (4)$$

### 4. Experimentations and results

The first important experimental work performed was the in-situ calibration of the measurement of the temperature of the sample contained in a container heated by the induction furnace. Then the metrological performances (sensitivity, linearity) of the heat flux calorimeter were characterised by using the calibration system incorporated permanently in the calorimeter. The new setup was then applied to the measurements of the enthalpy increments and enthalpy of fusion of some materials with well-known enthalpy variations as a function of temperature and the uncertainties for determination of specific heat were assessed.

#### 4.1. In-situ calibration of the sample temperature measurement

The pyrometer was initially calibrated in radiance temperature using reference blackbodies, but the radiative and thermal configurations when measuring the temperature of a sample inside the container heated in the induction furnace are very different from the conditions of the initial calibration. Indeed the container is heated by a graphite susceptor itself heated by the helical shaped heating inductive coil of the furnace. The inductive coil has four loops and is 60 mm high and the susceptor is 70 mm high. As the heating zone is quite short and the temperature is



Fig. 4. Specimen container design.



high, the heated parts (susceptor, container empty or with the sample) are submitted to very high local heat fluxes generating strong temperature non-homogeneities. Therefore, it was suspected that the mean temperature of the sample inside the container could be quite different from the one measured by the pyrometer on the bottom of the container. To quantify the errors on the sample mean temperature measurement, the pyrometer was calibrated in-situ with phase transition fixed points placed in the containers used for the enthalpy measurements. The principle of the in-situ calibration by phase transitions of fixed points was presented in [17] for the measurement of the sample temperature for thermal diffusivity configuration. The principle of the in-situ calibration consists in replacing the sample by a small crucible filled with a pure material or an eutectic alloy and to continuously measure the temperature with the pyrometer while heating or cooling the sample with a low heating rate until the material in the crucible is fully melted or frozen. The phase change is identified by a plateau of the temperature measured by the pyrometer versus time. Fig. 5 shows an example of the melting and freezing plateaus (seen by the pyrometer) because of the presence of copper in the specimen container during heating and cooling the crucible containing copper.

As the material is a pure material or an eutectic alloy the freezing or fusion occurs at a fixed known temperature. For the calibration, the sample is heated or let cooled with various heating or cooling rates and the error on the temperature measured by the pyrometer is extrapolated to the case where the heating or cooling rate is zero<sup>19</sup>. For the calibrations in temperature, pure copper with freezing point at 1084 °C and the two eutectic alloys Pt-C with melting temperature at 1738 °C and Ir-C with melting temperature at 2291 °C [18,19] were used. The copper and eutectic alloys were contained in graphite protecting crucibles to avoid pollution when metallic containers (tungsten, tantalum) were used. The results of in-situ calibrations of the sample temperature measurements are given in Table 1. The correction is the value to be added to the indicated temperature in order to get the corrected temperature. Results differ from one container to another with the same fixed points.

It is clear that the temperature calibration is a critical point as it differs from one container to another using the same fixed points and corrections are very significant especially at high temperatures.

#### 4.2. Characterisation of the linearity of the calorimeter

The linearity of the calorimeter was examined in isothermal conditions by measuring the sensitivity as a function of the energy dissipated inside the sample cell. The calorimeter was maintained at a constant temperature of 25 °C, and the sensitivity was determined for various power levels produced by the calibration system during a fixed dissipation time. Table 2 gives the sensitivity values, for four different amounts of energy ranging approximately from 50 J to 590 J dissipated during the dissipation time of 60 s. These results show a very small

**Table 1**

In-situ temperature calibration with different containers.

Container	Fixed point	Temperature indicated by the pyrometer (°C)	Correction (°C)
Tantalum	Cu	1087	−3
	Pt-C	1701	37
	Ir-C	2200	91
Graphite	Cu	1066	18
	Pt-C	1670	68
	Ir-C	2164	127
Tungsten	Cu	1053	31
	Pt-C	1658	80
	Ir-C	2158	133

**Table 2**

Thermopiles sensitivity as a function of dissipated energy.

Electrical energy dissipated (J)	Thermopiles sensitivity ( $\mu\text{V}\cdot\text{W}^{-1}$ )
51.67	49,209
206.84	49,234
465.43	49,238
589.98	49,253
Mean value	49,233
Relative standard deviation (%)	0.04

dependence of the sensitivity to the dissipated energy with a relative standard deviation on the four values less than 0.05%, and validate therefore the assumption of linearity of the calorimeter.

The influence of the dissipation time on the determination of the calorimeter sensitivity was also studied at 25 °C. The calorimeter was disconnected from the furnace and the atmosphere that fills the thermopiles was air (instead of helium when performing drops). This is why the sensitivity in these conditions is different from other sensitivities. Several tests were performed by releasing the same energy amount (about 586 J) in the sample cell for different dissipation times ranging from 60 to 300 s by adjusting the electrical current in the heater for each dissipation time. The results presented in Table 3 demonstrate the non-dependence of the sensitivity determination to the dissipation time, with a relative standard deviation on the seven values of sensitivity of about 0.03%.

#### 4.3. Measurement of the enthalpy of fusion of pure copper

Several shots of pure copper (6 N) from Goodfellow were put in a graphite container which was attached to the motorised gripper with a thin tantalum wire of 50  $\mu\text{m}$  diameter. In order to measure the enthalpy of fusion of copper, different drops were carried out for two samples (with mass of 2.0656 g and 3.4394 g respectively) heated at temperatures above and below the melting temperature. Enthalpy increments of the container and the sample are measured. Subtracting from these enthalpies' increments, the enthalpy increments of the graphite container leads to the enthalpy increments of the copper samples. The shift in the enthalpy increments at the temperature of fusion is due mainly to the enthalpy of fusion of copper.

**Table 3**

Thermopiles sensitivity as a function of the dissipation time.

Dissipation time (s)	Electrical energy dissipated (J)	Thermopiles sensitivity ( $\mu\text{V}\cdot\text{W}^{-1}$ )
60	588.99	49,423
120	585.65	49,418
180	583.66	49,419
240	583.88	49,395
300	589.19	49,387
Mean value		49,408
Relative standard deviation (%)		0.03

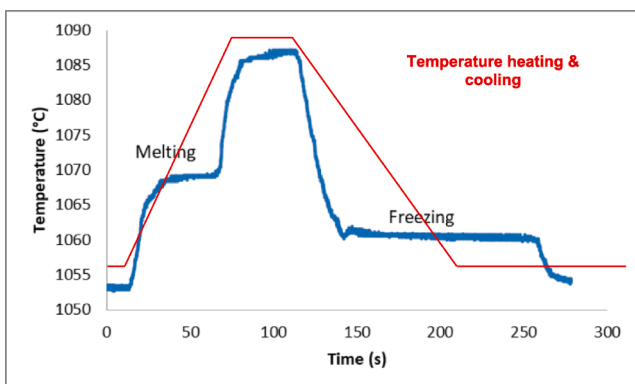


**Fig. 5.** Melting and freezing plateaus of Cu in graphite container.

Taking the molecular weight of copper as  $M(\text{Cu}) = 63.546 \text{ g}\cdot\text{mol}^{-1}$ , Tables 4 and 5 present the enthalpy increments of the two copper specimens. Fig. 6 shows the enthalpy increments of only the second copper sample of 3.4394 g. The temperature of the calorimetric block was maintained at 25 °C. The temperature of fusion measured (without correction) by the pyrometer is 1066 °C. The estimation of the enthalpy of fusion of copper is done using linear regression fits of the enthalpy increments at the solid phase and the liquid one.

The enthalpy of fusion of the specimen is considered as the gap, at the temperature of fusion, between the two regression lines of enthalpy increments of the solid and liquid states before and after the fusion.

Fitting enthalpy increments of copper samples before and after the temperature of fusion with two linear regressions and taking the shift at this temperature, the measured enthalpies of fusion for the two specimens of 2.0656 g and 3.4394 g are respectively  $12727.27 \text{ J}\cdot\text{mol}^{-1}$  and  $12743.58 \text{ J}\cdot\text{mol}^{-1}$ . These values are in good agreement with the value of  $(12928 \pm 277) \text{ J}\cdot\text{mol}^{-1}$  recommended by Stølen [6].

#### 4.4. Measurement of the specific heat of the $\alpha$ -alumina

A tantalum container with a height of 15 mm and a wire of tungsten 100  $\mu\text{m}$  in diameter were used to measure the specific heat of the  $\alpha$ -alumina (SRM 720 [20]). The mass of the  $\alpha$ -alumina specimen was 0.31745 g, and the mass of the tantalum container with the wire was 6.3640 g. Drops of empty and full container were done for four initial temperatures in the furnace and enthalpy increments were measured as presented in Table 6. The initial temperature of the container and container plus sample were corrected using the results of measurement of melting temperature of copper and Pt-C eutectic in the same tantalum container but with a thin graphite crucible for separation from tantalum. A linear correction of the temperature indicated by the pyrometer was applied using the two temperature calibration points.

A comparison between the measured differences in energy per gram at the four temperature points and the certified enthalpy increments of the SRM-720 is presented in Fig. 7. The molecular weight of the SRM-720 is  $M(\text{Al}_2\text{O}_3) = 101.9613 \text{ g}\cdot\text{mol}^{-1}$ .

Table 7 presents the comparison between the certified values of the specific heat of the SRM-720 and the values measured with the high temperature drop calorimeter of LNE. The relative deviation between the measured values and the certified ones is lower than 1.2% from 1200 °C to 1800 °C.

#### 4.5. Measurements of the specific heat of pure tungsten

The enthalpy increments of pure tungsten (99.95% purity from Goodfellow) were measured in the same way as for  $\alpha$ -alumina. The measurements were performed on a cylindrical specimen (10 mm height and 5 mm diameter) of 3.4826 g with a specimen container made of tungsten and a holding wire of tungsten (100  $\mu\text{m}$  in diameter). The overall mass of the empty container with the wire was 6.1502 g. Measurements were done in the temperature range 1200 °C to 2200 °C.

Electrical calibrations of the calorimeter sensitivity were performed after the drop of the specimen container in order to determine the

**Table 4**

Enthalpy increments of the first copper sample (2.0656 g).

Initial state of the copper	Temp. indicated by the pyrometer (°C)	Calorimeter sensitivity ( $\mu\text{V}\cdot\text{W}^{-1}$ )	Variation of enthalpy of the copper sample ( $\text{J}\cdot\text{mol}^{-1}$ )
Solid	1054	45,502	27863.77
	1034		27060.47
	1004		26130.15
	1014		26206.80
Liquid	1086	45,502	41469.61
	1105		41788.41
	1123		42308.39

**Table 5**

Enthalpy increments of the second copper sample (3.4394 g).

Initial state of the copper	Temp. indicated by the pyrometer (°C)	Calorimeter sensitivity ( $\mu\text{V}\cdot\text{W}^{-1}$ )	Variation of enthalpy of the copper sample ( $\text{J}\cdot\text{mol}^{-1}$ )
Solid	1057	45,495	28456.11
	1005		26745.99
	1014		26967.68
	1023		27200.65
	1037		27749.91
	1046		28009.61
Liquid	1131	45,495	43478.75
	1148		44073.48
	1112		42840.39
	1171		44817.12
	1093		42225.79

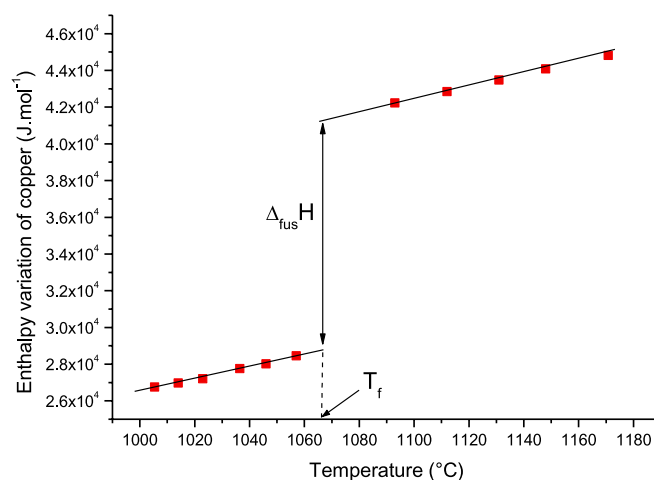


**Fig. 6.** Enthalpy increments of a copper sample ( $m = 3.4394 \text{ g}$ ).

sensitivity with the container and sample in the sample cell of the calorimeter. This way of proceeding ensured that the experimental conditions were similar as when measuring enthalpy of the container or container with sample. The electrical energy is chosen approximately equivalent to the order of magnitude of the enthalpy variation of the specimen and container.

Table 8 gives the results obtained on empty and full container for temperatures in the range from 1200 °C to 2200 °C.

This leads to the determination of the enthalpy increments of the tungsten specimen presented in Fig. 8 and compared with the literature values from NIST [23]. The molecular weight of tungsten is taken  $M(\text{W}) = 183.85 \text{ g}\cdot\text{mol}^{-1}$ .

Specific heat of the studied specimen is derived from the enthalpy increment's fitting curve. Table 9 presents the specific heat values determined by LNE and NIST [23,24] values in the studied temperature range. The maximum relative deviation between the specific heat of tungsten obtained by LNE and the data from NIST is 1.7% in the temperature range from 1200 °C to 2200 °C.

#### 4.6. Measurements of the specific heat of isotropic graphite IG210

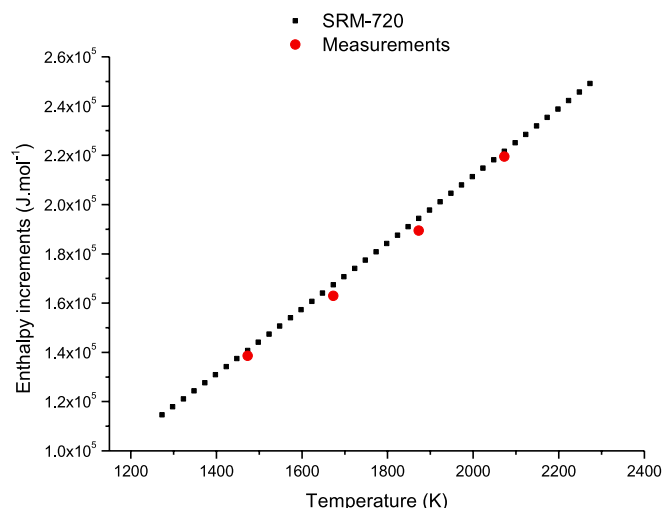
The specific heat of a high density isotropic graphite (IG210 from Toyo Tanso France) was determined by the above described method. The mass of the specimen (20 mm height and 5 mm in diameter) was 0.68936 g. The specimen was put in a high density graphite container and attached to the gripper with a tantalum fine wire (50  $\mu\text{m}$  in diameter). The mass of the empty container with the tantalum wire was 1.37371 g.

Tables 10 presents the enthalpy variations of the empty container

**Table 6**

Enthalpy increments obtained for empty tantalum container and for the tantalum container with the SRM-720 specimen.

	Temp. indicated by the pyrometer (°C)	Corrected temperature (°C)	Thermopiles sensitivity ( $\mu\text{V}\cdot\text{W}^{-1}$ )	Variation of enthalpy (J)
Empty container	1205	1210	45,470	1089
	1415	1433		1307
	1593	1623		1496
	1817	1862		1743
Full container	1204	1209	45,470	1523
	1418	1437		1831
	1594	1624		2098
	1817	1862		2458

**Fig. 7.** Comparison of the measured enthalpy increments with certified enthalpy increments of the SRM-720.**Table 7**

Comparison between the specific heat measured by LNE on SRM-720 and the certified values.

Temperature (K)	Specific heat measured by LNE ( $\text{J}\cdot\text{mol}^{-1}\cdot\text{K}^{-1}$ )	Specific heat - Certified value from NIST ( $\text{J}\cdot\text{mol}^{-1}\cdot\text{K}^{-1}$ )	Relative deviation from the certified value (%)
1473.15	130.41	131.98	-1.19
1673.15	132.77	134.06	-0.97
1873.15	135.00	135.67	-0.49
2073.15	137.14	136.94	0.14

and of the container with the graphite specimen for initial temperatures in the range 1000 °C to 2700 °C. The temperature of the calorimeter is always stabilised at 25 °C.

The specific heat obtained by differentiation of the enthalpy

**Table 8**

Enthalpy increments obtained for tungsten empty container and for the tungsten container with the tungsten specimen.

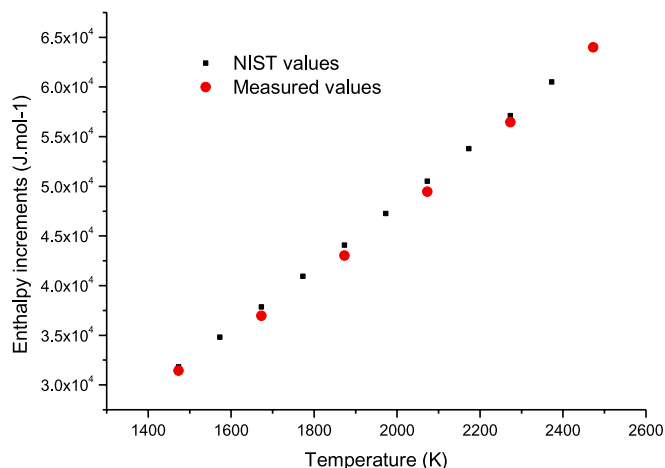
	Temp. indicated by the pyrometer (°C)	Corrected temperature (°C)	Thermopiles sensitivity ( $\mu\text{V}\cdot\text{W}^{-1}$ )	Variation of enthalpy (J)
Empty container	1196	1236	45,491	1084
	1410	1469		1290
	1613	1691		1491
	1822	1920		1751
	1991	2106		1932
	2194	2330		2153
Full container	1186	1226	45,491	1682
	1392	1449		2003
	1591	1667		2315
	1795	1891		2717
	1956	2068		3017
	2156	2288		3387

increments' curve is presented in Fig. 9.

#### 4.7. Uncertainty estimation of the specific heat measurements by the drop calorimeter

According to the measurement method, the uncertainty associated with the specific heat measurement are the combination of uncertainties associated with the following parameters:

- The mass of the specimen,
- The temperature of the specimen in the container,
- The temperature of the empty container before the drop,
- The temperature of the calorimeter,
- The sensitivity of the calorimeter,
- The enthalpy variations calculated from the signals delivered by the calorimeter,
- The mathematical model for fitting enthalpy increments of the specimen,

**Fig. 8.** Comparison of the measured enthalpy increments of tungsten with NIST values.



**Table 9**

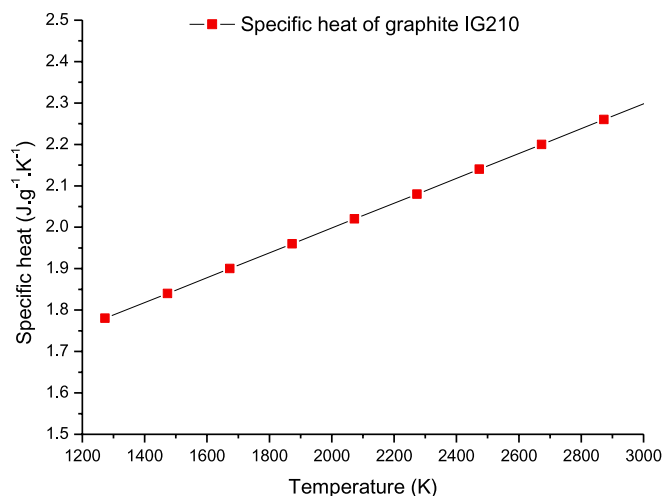
Comparison between the specific heat measured by LNE on tungsten and values from NIST.

Temperature (K)	Specific heat calculated from the measurements results ( $\text{J}\cdot\text{mol}^{-1}\cdot\text{K}^{-1}$ )	Certified value from NIST ( $\text{J}\cdot\text{mol}^{-1}\cdot\text{K}^{-1}$ )	Relative deviation from the certified value (%)
1473.15	29.5890	29.7411	-0.5
1673.15	30.6928	30.6869	0.0
1873.15	31.7985	31.6295	0.5
2073.15	32.9055	32.6496	0.8
2273.15	34.0133	33.5150	1.5
2473.15	35.1217	34.5345	1.7

**Table 10**

Enthalpy increments obtained for the empty graphite container and of the graphite container with the graphite specimen.

	Temperature indicated by the pyrometer ( $^{\circ}\text{C}$ )	Corrected temperature ( $^{\circ}\text{C}$ )	Thermopiles sensitivity ( $\mu\text{V}\cdot\text{W}^{-1}$ )	Variation of enthalpy (J)
Empty container	1025	1016	45,477	2188
	1192	1203		2615
	1403	1439		3196
	1595	1654		3743
	1809	1894		4030
	2014	2123		4562
	2200	2331		5036
	2387	2541		5546
Container and graphite sample	2546	2719	45,477	5919
	1039	1032		3329
	1203	1215		4002
	1417	1455		4907
	1605	1665		5743
	1805	1889		6283
	2017	2126		7201
	2201	2332		7947
	2392	2546		8799
	2554	2728		9374

**Fig. 9.** Measured specific heat of the isotropic graphite specimen IG210.

- The heat loss of the specimen during the drop and during the cooling in the calorimeter.

The standard uncertainties of these different parameters are estimated in the case of the determination of the specific heat of a sample of  $\alpha$ -alumina (SRM-720). They are detailed in the following parts.

- Uncertainty associated with the measurement of the mass of the sample

The uncertainty associated with the measurement of the mass of the tested specimen is a combination of several uncertainty sources including the linearity, the resolution, the calibration, the repeatability and the reproducibility of the used balance. It has been estimated to be equal to 0.12 mg as a standard uncertainty.

- Uncertainty associated with the temperature of the specimen

The uncertainty associated with the temperature of the specimen is estimated during the temperature calibration process to be equal to  $\pm 6^{\circ}\text{C}$ . A rectangular probability distribution associated with this temperature uncertainty leads to the standard uncertainty:

$$u_c(T_{Full}) = \left( \frac{7}{\sqrt{3}} \right) = 4^{\circ}\text{C}$$

- Uncertainty associated with the temperature of the empty container

The uncertainty associated with the temperature of the empty container is also estimated to be equal to the uncertainty associated with the temperature of the specimen during the temperature calibration process to be equal to  $\pm 6^{\circ}\text{C}$ . A rectangular probability distribution associated with this temperature uncertainty leads to the standard uncertainty:

$$u_c(T_{Empty}) = \left( \frac{7}{\sqrt{3}} \right) = 4^{\circ}\text{C}$$

- Uncertainty associated with the temperature of the calorimeter

The temperature of the calorimeter maintained at  $25^{\circ}\text{C}$  is measured using a calibrated Pt-100 thermometer. This temperature is maintained within  $0.1^{\circ}\text{C}$  and the uncertainty associated with the temperature of the calorimeter before the drop of the sample has no significant effect on the measurement of enthalpy increments. This uncertainty will be neglected in the uncertainty budget.

- Uncertainty associated with the areas of the peaks of empty and full container drops

The uncertainty associated with the areas of the peaks of empty and full container drops is estimated from the influence of the integration limits and the base line selection. Taking different integration limits with a linear baseline calculation mode, the relative uncertainty is estimated to be better than 0.1%. This uncertainty will be maximised by taking:

$$\frac{u_c(A)}{A} = 0.1\%$$

- Uncertainty associated with the sensitivity of the calorimeter

The sensitivity of the calorimeter  $\beta$  at its near ambient temperature ( $25^{\circ}\text{C}$  maintained using a temperature regulated water jacket) is calculated by:

$$\beta = \frac{A_c}{E} \quad (5)$$

With  $A_c$ : The area of the calibration peak, and  $E$  the corresponding released electrical energy.

The electrical energy is measured, by the two electrical voltage drops over the heater and over the standard resistance in addition to the dissipation time, with an uncertainty of about 0.06%. The area of the

corresponding peak is measured with an uncertainty of about 0.1%. This leads to the determination of the sensitivity of the calorimeter with a standard relative uncertainty of about 0.12%.

- Uncertainty associated with the mathematical model for fitting enthalpy increments of the specimen.

The mathematical models for fitting enthalpy increments (expressed in Joule) of empty and full container is given previously in equation (3).

The deviation of the fitting curve from experimental measurements varies between  $-0.70\%$  and  $0.69\%$ . This deviation is more important than the uncertainty associated with individual uncertainty on the measured enthalpy increments; which is about 0.16% taking in account the uncertainties associated with the sensitivity (0.12%) and the areas of the drop peaks (0.1%).

A rectangular probability distribution associated with this fitting uncertainty leads to the standard uncertainty of the mathematical model:

$$u_c(\Delta H_{\text{Fitting}}) = \left( \frac{0.7\%}{\sqrt{3}} \right) = 0.4\%$$

This uncertainty will be associated with the specific heat fitting, which is the differentiation of this mathematical model.

- Uncertainty associated with the heat loss of the specimen during its drop and after it.

A comparison between the measured differences in energy per gram at the four temperature points and the certified enthalpy increments of the SRM-720 was shown in Fig. 6. According to this figure, the measurements of enthalpy increments of the certified reference material  $\alpha$ -alumina (SRM-720) gave a deviation from the certified enthalpy increments from  $-2.58\%$  to  $-0.96\%$ . This leads to a mean heat loss correction of about 1.7% on the enthalpy increments. This heat loss correction is not applied to enthalpy increments, but it is directly included in the estimation of the uncertainty associated with the specific heat.

- Uncertainty budget on the measurement of specific heat of SRM-720

The final relative expanded uncertainty of the specific heat determination is given by:

$$\frac{U(c_p)}{c_p} = 3.5\%$$

With a reported result (given as an example at  $1600^\circ\text{C}$ )

$$c_p = (1.324 \pm 0.047) \text{ J}\cdot\text{g}^{-1}\cdot\text{K}^{-1}$$

At the moment, the uncertainty on specific heat measurements of other materials than SRM 720 exceeds this relative expanded uncertainty of 3.5% evaluated for the sapphire, especially at higher temperatures.

## 5. Conclusion

LNE-LCM has adapted its homemade high temperature Laser Flash Apparatus in order to measure enthalpy increments by drop calorimetry and to determine specific heat of solid materials at high temperatures. The correct technical operation of the installation has been demonstrated up to  $2700^\circ\text{C}$ . The measurement of the sample temperature in the induction furnace was calibrated by using three fixed points melting from  $1084^\circ\text{C}$  to  $2291^\circ\text{C}$ . The calibrations gave large corrections for the temperature indicated by the pyrometer and at this stage, the assessment of the uncertainty on the sample temperature in the furnace is difficult and remains provisional.

The global validations of specific heat measurement on two materials with known specific heats (alumina, pure tungsten) showed that from  $1200$  to  $2200^\circ\text{C}$ , the specific heat measurements with the prototype setup with induction furnace can be done with a relative uncertainty of a few percent (less than 5%). However, it must be noticed that those results are obtained with significant temperature corrections for the sample temperature in the furnace before the drop. Due to the large sample temperature corrections, the accurate assessment of uncertainties on the measured specific heat is difficult.

The next step for improving the uncertainties will be to improve the furnace or use another furnace. Indeed, the uncertainty on the mean sample temperature in the furnace before the drop in the calorimeter is mostly due to the difficulty to measure the temperature of the container by pyrometry and to the non-uniformities of the temperatures of the sample and of the container. The non-uniformities of the temperatures are due to the very high radiation heat fluxes at high temperatures accentuated by the very large opening of the furnace that does not constitute an isothermal enclosure around the container with the sample.

## CRedit authorship contribution statement

**Refat Razouk:** Conceptualization, Methodology, Data curation, Formal analysis, Writing – Original draft preparation, Writing – review & editing **Olivier Beaumont:** Validation, Investigation. **Jacques Hameury:** Writing – review & editing. **Bruno Hay:** Supervision.

## Declaration of Competing Interest

The authors declare that they have no known competing financial interests or personal relationships that could have appeared to influence the work reported in this paper.

## Acknowledgements

This project 17IND11 Hi-TRACE has received funding from the EMPIR programme co-financed by the Participating States and from the European Union's Horizon 2020 research and innovation programme.

## References

- [1] D.A. Ditmars, Drop calorimetry above 300 K, in: A. Cezairliyan (Ed.), *Specif Heat of Solids*, Hemisphere Pub. Corp., 1988, pp. 243–261.
- [2] D.C. Ginnings, Precision Measurement and Calibration, NBS, U.S. Government Printing Office, 1970.
- [3] Y.S. Touloukian, E.H. Buyco, Thermophysical Properties of Matter - The TPRC Data Series. Volume 4. Specific Heat - Metallic Elements and Alloys, 1971. IFI/Plenum.
- [4] B. Legendre, D. Girolamo, P. Le Parlouer, B. Hay, Détermination des capacités thermiques en fonction de la température par calorimétrie de chute, *Rev. Française Métrologie*. 1 (2006) 23–30.
- [5] F. Schubert, M. Gollner, J. Kita, F. Linseis, R. Moos, First steps to develop a sensor for a Tian – Calvet calorimeter with increased sensitivity, *J. Sensors Sensor Syst.* (2016) 205–212, <https://doi.org/10.5194/jsss-5-205-2016>.
- [6] S. Stølen, F. Grønvold, Critical assessment of the enthalpy of fusion of metals used as enthalpy standards at moderate to high temperatures, *Thermochim. Acta*. 327 (1–2) (1999) 1–32.
- [7] V.Y. Chekhovskoy, Levitation calorimetry, in: K.D. Maglic, A. Cezairliyan, V. E. Peletsky (Eds.), *Compend. Thermophys. Prop. Meas. Methods 1. Surv. Meas. Tech.*, Plenum Press, New York, 1984, p. 789.
- [8] M.B. Ouaida, J.M. Badie, Aerodynamic levitation apparatus coupled with solar furnace for study of matter in the liquid state, *J. Phys. E*. 15 (9) (1982) 941–944, <https://doi.org/10.1088/0022-3735/15/9/021>.
- [9] S.V. Ushakov, A. Navrotsky, D.J. Green, Experimental approaches to the thermodynamics of ceramics above  $1500^\circ\text{C}$ , *J. Am. Ceram. Soc.* 95 (5) (2012) 1463–1482, <https://doi.org/10.1111/j.1551-2916.2012.05102.x>.
- [10] B. Hay, J. Hameury, N. Fleurence, P. Lacipiere, M. Grelard, V. Scaerac, G. Davee, New facilities for the measurements of high-temperature thermophysical properties at LNE, *Int. J. Thermophys.* 35 (9–10) (2014) 1712–1724, <https://doi.org/10.1007/s10765-013-1400-8>.
- [11] W.J. Parker, R.J. Jenkins, C.P. Butler, G.L. Abbott, Flash Method of Determining Thermal Diffusivity, Heat Capacity, and Thermal Conductivity, *J. Appl. Phys.* 32 (9) (1961) 1679–1684, <https://doi.org/10.1063/1.1728417>.

- [12] K. Boboridis, B. Hay, Improved metrology of thermophysical properties at very high temperatures The EMPIR project Hi-TRACE, *Atw Int. Zeitschrift Fuer Kernenergie*. 65 (2020) 140–141. [http://inis.iaea.org/search/search.aspx?orig\\_q=RN:51070413](http://inis.iaea.org/search/search.aspx?orig_q=RN:51070413).
- [13] E. Calvet, H. Prat, *Microcalorimétrie: applications physicochimiques et biologiques.*, Masson, Paris, 1956.
- [14] E. Calvet, *Récents progrès en microcalorimétrie*, Dunod, Paris, 1958.
- [15] R. Razouk, B. Hay, M. Himbert, A new in situ electrical calibration system for high temperature Calvet calorimeters, *Rev. Sci. Instrum.* 84 (9) (2013) 094903, <https://doi.org/10.1063/1.4821876>.
- [16] R. Razouk, B. Hay, M. Himbert, Uncertainty assessment of enthalpy of fusion measurements performed by using an improved Calvet calorimeter, *Metrologia*. 52 (5) (2015) 717–729, <https://doi.org/10.1088/0026-1394/52/5/717>.
- [17] G. Failleau, et al., Metal-carbon eutectic high temperature fixed points for in-situ calibration of radiation thermometers, *High Temp. - High Press.* 50 (2021) 149–165, <https://doi.org/10.32908/hthp.v50.1013>.
- [18] Y. Yamada, H. Sakate, F. Sakuma, A. Ono, High-temperature fixed points in the range 1150 °C to 2500 °C using metal-carbon eutectics, *Metrologia*. 38 (2001) 213–219, <https://doi.org/10.1088/0026-1394/38/3/3>.
- [19] H. Preston-Thomas, The International Temperature Scale of (ITS-90), *Metrologia*. 27 (1990) (1990) 3–10, <https://doi.org/10.1088/0026-1394/27/1/002>.
- [20] G.A. Uriano, National Bureau of Standards Certificate - Standard Reference Material 720 Synthetic Sapphire (a-Al<sub>2</sub>O<sub>3</sub>), (1982) 3.
- [21] V.A. Bychinskii, A.A. Tupitsyn, A.V. Mukhetdinova, K.V. Chudnenko, S. V. Fomichev, V.A. Krenev, Estimation of the heat capacity of individual substances on the basis of experimental enthalpy increments, *Russ. J. Inorg. Chem.* 58 (9) (2013) 1079–1084, <https://doi.org/10.1134/S0036023613090040>.
- [22] M.A. Sineva, I.V. Morozov, G.V. Belov, N.M. Aristova, Y.a. Lavrinenko, Simultaneous analysis of the enthalpy increment and heat capacity data measurements for updating the IVTANTHERMO database, *J. Phys. Conf. Ser.* 1385 (2019) 012025, <https://doi.org/10.1088/1742-6596/1385/1/012025>.
- [23] J. Chase, M.W., NIST-JANAF Thermochemical Tables, Fourth Edition, *J. Phys. Chem. Ref. Data, Monogr.* 9. (1998) 1–1951.
- [24] NIST, tungsten, (n.d.). <https://webbook.nist.gov/cgi/cbook.cgi?ID=C7440337&Type=JANAFS&Plot=on#JANAFS> (accessed March 31, 2020).